HHS Public Access

Author manuscript

Oncogene. Author manuscript; available in PMC 2020 July 20.

Published in final edited form as:

Oncogene. 2020 March ; 39(11): 2424–2436. doi:10.1038/s41388-020-1159-x.

GRK2 Enforces Androgen Receptor-Dependence in the Prostate and Prostate Tumors

Adam J. Adler[1], **Payal Mittal**[1,5], **Adam T. Hagymasi**[1,6], **Antoine Menoret**[1], **Chen Shen**[1], **Federica Agliano**[1], **Kyle T. Wright**[1], **James J. Grady**[2], **Chia Ling Kuo**[2], **Enrique Ballesteros**[3], **Kevin P. Claffey**[4], **Anthony T. Vella**[1]

[1]Department of Immunology, School of Medicine, UConn Health, Farmington, CT, USA

[2]Department of Community Medicine and Health Care, School of Medicine, UConn Health, Farmington, CT, USA

[3]Department of Pathology and Laboratory Medicine, School of Medicine, UConn Health, Farmington, CT, USA

[4]Department of Cell Biology, School of Medicine, UConn Health, Farmington, CT, USA

[5]Present address: Merck Research Laboratories, Oncology Department, Boston, MA, 02115

[6]Present address: Carole and Ray Neag Comprehensive Cancer Center, University of Connecticut School of Medicine, Farmington, CT, USA

Abstract

Metastatic tumors that have become resistant to androgen deprivation therapy represent the major challenge in treating prostate cancer. Although these recurrent tumors typically remain dependent on the androgen receptor (AR), non-AR-driven tumors that also emerge are particularly deadly and becoming more prevalent. Here, we present a new genetically engineered mouse model for non-AR-driven prostate cancer that centers on a negative regulator of G protein-coupled receptors that is downregulated in aggressive human prostate tumors. Thus, prostate-specific expression of a dominant-negative G protein-coupled receptor kinase 2 (GRK2-DN) transgene diminishes AR and AR target gene expression in the prostate, and confers resistance to castration-induced involution. Further, the GRK2-DN transgene dramatically accelerates oncogene-initiated prostate tumorigenesis by increasing primary tumor size, potentiating visceral organ metastasis, suppressing AR, and inducing neuroendocrine marker mRNAs. In summary, GRK2 enforces AR-dependence in the prostate, and the loss of GRK2 function in prostate tumors accelerates disease progression towards the deadliest stage.

Correspondence: Adam J. Adler, Department of Immunology, School of Medicine, UConn Health, Farmington, CT 06030-1319, USA, phone: (860) 679-7992, aadler@uchc.edu; Anthony T. Vella, Department of Immunology, School of Medicine, UConn Health, Farmington, CT 06030-1319, USA, phone: (860) 679-4364, vella@uchc.edu.

Conflict of interest

The authors declare that they have no conflict of interest.

Introduction

Cancer in American men occurs most commonly in the prostate [1]. Primary tumors can be effectively treated with surgery or radiation, but metastatic disease is incurable [2]. Androgen deprivation therapy (ADT) using androgen receptor (AR) antagonists or androgen synthesis modulators typically achieves remission, however, castration-resistant prostate cancer (CRPC) invariably develops. This can occur through selection of tumors with mutations or isoforms in the AR or other factors that activate AR-downstream signaling [3]. For instance, AR splice variants lacking the ligand binding domain are constitutively active [4].

The most aggressive form of CRPC, however, downregulates AR and becomes less dependent on the AR signaling axis, while sometimes upregulating neuroendocrine markers [5–7]. Although AR^{low} neuroendocrine prostate cancer (NEPC) cells are only present in isolated foci of “hormone naïve” tumors, and full-blown NEPC has historically only been diagnosed in a minority of patients, the incidence of therapy-induced $AR^{neg}NE^{+}$ (NEPC) as well as $AR^{neg}NE^{neg}$ prostate tumors have increased with the wide spread use of the newest generation of potent ADT drugs enzalutamide and abiraterone [7–10]. Further, in contrast to AR-driven metastasis that are generally only found in draining lymph nodes (LN) and bone, non-AR-driven metastasis also have a propensity to form in visceral organs that are associated with the poorest prognosis and lack of response to chemo and immune checkpoint therapies [5, 11–15].

Although AR-driven CRPC has been well studied [3], the more aggressive non-AR-driven forms of CRPC such as NEPC have only begun to be analyzed [6, 7, 10, 16, 17]. It has been shown that AR directly represses a critical driver of neuroendocrine transdifferentiation [18], suggesting that AR downregulation precipitates subsequent disease progression. Revealing how prostatic AR is suppressed will thus likely be important for understanding the etiology of, as well as developing therapies for the most aggressive forms of prostate cancer.

Prostate tumorigenesis involves numerous genetic and biochemical events that initiate transformation, metastasis, transition to castration-resistance and neuroendocrine transdifferentiation. Two commonly used genetically engineered mouse models develop primary prostate tumors either from the expression of the SV40 large T antigen in the prostate [19] that blocks the tumor suppressors p53 and RB1 whose losses are associated with human prostate cancer [20, 21], or deleting the PTEN tumor suppressor [22] whose loss represents the most frequent genetic alteration in human prostate cancer [23]. The large T antigen-expressing TRAMP mice have been instrumental in studying prostate tumorigenesis [24] and its impact on immune function [25–27], and also facilitated pre-clinical development of immune checkpoint therapy [28]. Additionally, the conditional $Pten^{-/-}$ model revealed a critical role for PTEN in enforcing castration-sensitivity [29, 30]. Metastasis in both the conditional $Pten^{-/-}$ model as well as in TRAMP mice (depending upon the genetic background [31, 32]) is typically low, but can be increased by introducing various second genetic hits [33]. Also, metastasis often tend to localize in LN rather than distant sites associated with poor patient prognosis [11, 12]. Further, it is generally unknown in many models whether metastasis become non-AR-driven [33].

G protein-coupled receptors (GPCR) that bind chemokines and other ligands regulating cell motility are linked to disease progression and metastasis in prostate and other cancers [34–39]. Nevertheless, metastasis form in most previous mouse prostate cancer models by targeting mitogenic or cell cycle regulators (e.g., [40–44]). Here, we targeted G protein-coupled receptor kinase 2 (GRK2), a negative regulator of GPCRs [45, 46] that is emerging as a regulator of disease progression in various cancers [47–53]. In particular, GRK2 expression is diminished in human prostate tumors with the highest Gleason scores [54].

To assess how diminished GRK2 function impacts prostate tumorigenesis, we constructed a novel transgenic mouse expressing a dominant-negative GRK2 (GRK2-DN) [55] in prostate epithelia. Although these GRK2-DN mice did not develop prostate tumors, GRK2-DN × TRAMP double transgenic (G2-TP) mice developed primary tumors that were substantially larger than TRAMP. G2-TP mice also developed metastasis at a much higher frequency, which often localized to visceral organs. G2-TP primary tumors and metastasis also exhibited diminished expression of AR and AR target genes, along with increased expression of mRNAs that encode neuroendocrine markers. Strikingly, GRK2-DN single transgenics also exhibited reduced AR and AR target gene expression despite the absence of tumor formation, and were more resistant to castration-induced prostate involution compared to wild-type mice. This study thus reveals an unexpected role for GRK2 in supporting AR expression and enforcing AR-dependence in the prostate, and further demonstrates that diminished GRK2 function in prostate tumors accelerates disease progression towards a highly aggressive non-AR-driven stage.

Results

GRK2 blockade accelerates prostate tumorigenesis

Given the plethora of GPCRs that might regulate prostate tumorigenesis [34–39], we sought to globally disinhibit prostatic GPCRs in order to amplify the tumor-promoting effects of ambient GPCR ligands, and hence reveal natural disease progression pathways.

GPCR signaling is tightly controlled. Ligand induces GPCR phosphorylation by G protein-coupled receptor kinase 2 (GRK2) that enables attachment of β-arrestin and subsequent disruption of G protein activation [45, 46]. Importantly, GRK2 is emerging as a regulator of tumor progression [47]. For instance, blocking GRK2 augments HEK tumor growth [48], and reciprocally augmenting GRK2 function inhibits thyroid tumor growth [49]. Further, inflammation increases hepatocellular carcinoma cell proliferation, invasion and migration by downregulating GRK2 [50], Kaposi’s sarcoma-associated herpesvirus can induce tumorigenesis via miRNA-mediated GRK2 downregulation [51], and the lncRNA UCA1 promotes gastric tumor metastasis by inducing GRK2 ubiquitination and degradation [53]. In relation to prostate cancer, the tumor-forming potential of the castration-resistant human prostate tumor cell line PC-3 is diminished by directly blocking G protein signaling (that is naturally inhibited by GRK2) [52]. Further, GRK2 expression inversely correlates with Gleason score in primary human prostate tumors [54].

To assess whether blocking the ability of prostatic GRK2 to regulate GPCR signaling impacts tumorigenesis, a cDNA encoding a dominant-negative GRK2 (GRK2-DN) that

blocks β-arrestin engagement and thus enhances GPCR signaling [55] was placed under the control of the prostate-specific ARR_2PB small composite probasin promoter [56] (Fig. 1a). The resulting PB-GRK2-DN transgene cassette was then microinjected into fertilized C57BL/6 embryos. Since prostate tumors that develop in TRAMP mice on the pure C57BL/6 genetic background grow more slowly and are less prone to metastasis and neuroendocrine transdifferentiation compared to the FVB or C57BL/6 × FVB F1 backgrounds [31, 32, 57], we reasoned that expressing the PB-GRK2-DN transgene on the pure C57BL/6 background would enable us to more readily assess its capacity to augment SV40 T antigen-induced tumorigenesis (see below). Nevertheless, PB-GRK2-DN transgenic (Tg) males (referred to hereafter as “GRK2-DN”) were fertile, and none (of >31 examined) exhibited increased prostate weight (not shown).

Canonical GPCR signaling involves activation of G proteins, then adenylyl cyclase that produces cAMP, then phosphorylation of protein kinase A (PKA) that activates/phosphorylates the transcription factor cAMP response element binding protein (CREB) [45, 58]. Western blot analysis revealed that GRK2-DN prostates expressed more phosphorylated CREB (pCREB, normalized to total CREB) as well as phosphorylated PKA catalytic domain (pPKA C, normalized to β-tubulin) compared to age-matched WT prostates (Fig. 1b–c, $p < 0.05$ for each). Additionally, while immunohistochemical (IHC) analysis of WT prostates revealed minimal nuclear pCREB staining in some stromal cells (blue arrow) and basal (red arrow) but not luminal epithelium (Fig. 1d, top panel), GRK2-DN prostates displayed robust nuclear pCREB immunoreactivity in luminal epithelial cell patches (black arrows, Fig. 1d, bottom panel). Taken together, the GRK2-DN transgene appears to disinhibit canonical GPCR-G protein signaling in the prostate, but this alone fails to initiate tumorigenesis.

Despite the absence of tumor formation in GRK2-DN single-Tg mice, GRK2-DN × TRAMP double Tg mice on the pure C57BL/6 background (hereafter referred to as “G2-TP”) exhibited accelerated tumor progression compared to pure C57BL/6 single-Tg TRAMP. Specifically, G2-TP primary (1°) tumors generally became palpable several months earlier than TRAMP (Fig. 2a), and average 1° tumor weight at necropsy was 2.5-fold greater in G2-TP compared to TRAMP ($p < 0.0001$ adjusted for age, Fig. 2b). Although the gross morphology of the 1° tumors varied somewhat within each strain, TRAMP tumors (vertical arrow, Fig. 2c) tended to cause seminal vesicle distension (horizontal arrows, Fig. 2c). In contrast, even though pure C57BL/6 G2-TP tumors often became very large (arrow in Fig. 2d), they did not typically distend the seminal vesicles, a pattern previously observed in C57BL/6 × FVB F1 single-Tg TRAMP mice [57]. Second, while metastasis (abbreviated as “Mets” in the figures) were detected in only 3/39 (8%) single-Tg TRAMP mice (closed circles in Fig. 2a, 3a) that only localized to LN (100%), metastasis or invasive primary tumors (i.e., that had fused with surrounding abdominal organs) were detected in 33/58 (57%) G2-TP mice (closed triangles in Fig. 2a, 3a). Tumor nodules were never detected in female G2-TP mice (0/21, aged 6–13 months). Male G2-TP metastasis localized in either LN (21 mice) or visceral organs such as the liver and lung (13 mice) (Fig. 3b, c). Thus, metastasis not only occurred at a much higher frequency in G2-TP mice (Figs. 2a, 3a), but only G2-TP metastasis localized to visceral organs (Fig. 3b). Metastasis in the liver (most frequent visceral organ site) stained robustly for the proliferation marker Ki67, in contrast to

surrounding liver parenchyma that only exhibited sporadic Ki67 immunoreactivity (Fig. 3d) and normal prostate where Ki67 was only observed in what appear to be basal epithelial cells (Fig. 3e, arrow).

H & E sections of G2-TP liver metastasis were scored as having a moderately differentiated adenocarcinoma morphology (i.e., some preserved glandular structure, arrow in Fig. 3f), suggesting that they may migrate at an early stage of tumorigenesis. Nevertheless, the overall difference in tumor development between GRK2-DN, TRAMP and G2-TP mice clearly indicates that although blocking prostatic GRK2 is not sufficient to initiate tumorigenesis, it dramatically potentiates oncogene-induced tumor progression.

GRK2 supports prostatic AR

To unravel how diminished GRK2 function accelerates tumorigenesis, qRT-PCR was performed on prostates, 1° tumors and metastasis (Fig. 4). As expected, Ki67 expression was generally high in TRAMP and G2-TP 1° tumors as well as in G2-TP LN and liver metastasis, but near baseline in non-Tg (WT) and GRK2-DN single-Tg prostates (Fig. 4a). Primers to the 3'UTR common to both the TRAMP and GRK2-DN transgenes confirmed that most 1° TRAMP tumors expressed the oncogene SV40 T antigen (Fig. 4b), although expression of the GRK2-DN transgene was very low in GRK2-DN single-Tg prostates (Fig. 4b). This was surprising given that the GRK2-DN transgene accelerates T antigen-initiated tumorigenesis (Figs. 2, 3). Further, the combined expression of both the T antigen and GRK2-DN transgenes in 1° G2-TP tumors trended lower compared to T antigen expression in TRAMP 1° tumors, and also trended lower in G2-TP LN and, to a lesser extent, liver metastasis (Fig. 4b). Finally, although there was a positive correlation between transgene expression and 1° tumor weight in both TRAMP (r squared value (r^2) = 0.82, $p = 0.005$) and G2-TP ($r^2 = 0.78$, $p = 0.004$) mice, transgene expression was relatively low even in very large 1° G2-TP tumors (Fig. 4c).

Given the centrality of AR to both normal prostate function and tumorigenesis [59], and that the probasin promoters driving both T antigen (in TRAMP) [60] and GRK2-DN [56] are AR-dependent, we considered the possibility that differences in transgene expression as well as tumor progression in TRAMP versus G2-TP mice might be associated with altered AR expression. Similar to transgene expression (Fig. 4b), AR mRNA expression trended lower in both G2-TP 1° tumors and liver metastasis compared to TRAMP 1° tumors and was virtually absent in G2-TP LN metastasis (Fig. 4d). Further, in TRAMP 1° tumors AR positively correlated with both transgene mRNA ($r^2 = 0.98$, $p < 0.0001$, Fig. 4e) and tumor weight ($r^2 = 0.86$, $p = 0.003$, Fig. 4f). In contrast, AR and transgene mRNAs did not significantly correlate in G2-TP 1° tumors, liver or LN metastasis ($r^2 = 0.41$, 0.21, and 0.49, respectively, Fig. 4e), and although there was a significant correlation between AR expression and G2-TP 1° tumor weights ($r^2 = 0.80$, $p = 0.003$), the slope of the linear regression was 14-fold less steep compared to TRAMP (Fig. 4f). Interestingly, AR expression also trended lower in GRK2-DN single-Tg compared to non-Tg prostates (Fig. 4d).

These data suggested that blocking prostatic GRK2 suppresses AR. To determine if the reductions in AR mRNA were actually associated with diminished AR function, expression

of several androgen-responsive target genes were measured by qRT-PCR (Fig. 5). For instance, expression of the clinically relevant tumor suppressor Nkx3.1 [61–63] was similar to AR in that it trended lower in G2-TP compared to TRAMP 1° tumors, was near baseline in G2-TP LN metastasis, and slightly elevated in G2-TP liver compared to LN metastasis (Fig. 5, left top panel). That Nkx3.1 mRNA expression also trended lower in GRK2-DN prostates (that do not express elevated Ki67 (Fig. 4a) or form tumors (Fig. 1d)) compared to WT further suggested that diminished GRK2 function may activate clinically relevant pathways capable of accelerating disease progression when transformation is initiated by a separate oncogenic event. Nevertheless, additional evidence that the GRK2-DN transgene diminishes AR activity in the prostate was provided by the expression patterns of the androgen-responsive gene *Tmprss2* [64] as well as the chemokine receptor CXCR4 that has been linked to AR signaling [65] (Fig. 5, left middle and bottom panels) that were both comparable to AR, transgene and Nkx3.1. Finally, the correlation between AR and its targets (linear regression analyses shown on the right side of Fig. 5) was consistently strong in TRAMP primary 1° tumors that expressed the highest amounts of AR ($r^2 = 0.98–0.99$, $p < 0.0001$), moderate in G2-TP 1° tumors and liver metastasis where AR was expressed at intermediate amounts (r^2 ranged from 0.45 to 0.94 and p ranged from 0.01 to non-significant), and the weakest in G2-TP LN metastasis that expressed minimal AR (r^2 ranged from 0.15 to 0.92 and p was non-significant in all cases). Thus, although AR expression varied somewhat between samples in most treatment groups, the trend in reduced AR expression in G2-TP 1° tumors and metastasis correlated with reduced AR target gene expression at the level of individual samples. These androgen target gene expression patterns (Figs. 4E and 5) are thus consistent with a role for GRK2 in supporting AR function.

Blockade of prostatic GRK2 function programs a non-AR-driven phenotype

AR-driven CRPC can be programmed by gain-of-function mutations in enzymes that convert adrenal precursors into the most potent form of androgen, dihydrotestosterone (DHT), that enables continued AR activation when testes-derived testosterone is blocked [66, 67]. This does not appear to be the case in GRK2-DN mice, however, since expression of both AR (Fig. 4d) and AR target genes are reduced (Fig. 5). To further explore this possibility, expression of the genes encoding two isoforms of the DHT-synthesizing enzyme steroid-5α-reductase were compared (Fig. 6). Thus, transition of human prostate tumors to castration-resistance can be associated with a shift from isoenzyme-2 (encoded by *Srd5a2*) that converts testes-derived testosterone to DHT towards isoenzyme-1 (encoded by *Srd5a1*) that generates DHT from adrenally-supplied androstenedione [66]. Expression of SRD5A2 mRNA (castrate-sensitive) was highest in WT prostate, but progressively decreased in single-Tg GRK2-DN prostate, TRAMP 1° tumors, G2-TP 1° tumors and finally G2-TP LN and liver metastasis where it was undetectable (Fig. 6, top panel). This downward trend in *Srd5a2* expression with advancing disease stage ($p < 0.0001$, TrendTest) suggested that diminished GRK2 function facilitates testosterone-independent disease progression. Importantly, expression of SRD5A1 mRNA (castrate-resistant) did not increase with disease stage, except for a slight (statistically non-significant) increase in G2-TP liver metastasis (Fig. 6, bottom panel), suggesting that disease progression also does not rely on adrenally-derived DHT precursor.

Rather, this result (Fig. 6) in concert with the loss of AR and AR target gene expression (Figs. 4d, 5) suggested that G2-TP tumors are non-AR-driven. NEPC, the best characterized form of non-AR-driven CRPC, expresses neuroendocrine markers such as Aurora Kinase A, Chromogranin A and synaptophysin [6]. WT and single-Tg GRK2-DN prostates expressed negligible mRNA for all three neuroendocrine markers (Fig. 7). TRAMP 1° tumors expressed Aurora Kinase A mRNA, while synaptophysin and Chromogranin A mRNAs were each detected in 3 of 7 samples. This expression pattern is consistent with a previous analysis of TRAMP mice reporting that neuroendocrine transdifferentiation, in particular synaptophysin expression, is a stochastic late stage event in tumorigenesis [68]. Notably, Aurora Kinase A mRNA expression trended higher in G2-TP compared to TRAMP 1° tumors, while Chromogranin A and synaptophysin mRNAs were significantly increased in G2-TP 1° tumors ($p < 0.05$ for both). G2-TP LN and liver metastasis also expressed all three neuroendocrine marker mRNAs, albeit expression was more consistent in the LN metastasis (Fig. 7), tracking with the lower AR expression in LN compared to liver metastasis (Fig. 4d).

The loss of prostatic GRK2 function confers castration-resistance irrespective of transformation

The overall disease pattern in G2-TP mice – metastasis colonization in visceral organs (Fig. 3), diminished expression of AR (Fig. 4d), AR target genes (Fig. 5) and 5α-reductase (Fig. 6), along with increased neuroendocrine marker mRNAs (Fig. 7) – suggested that GRK2 may normally support prostatic AR, and conversely that diminished GRK2 function in prostate tumors facilitates non-AR-driven disease. To test this, tumor development was compared in G2-TP versus TRAMP single-Tg mice that were castrated or sham-operated (control) at 4 months of age and then necropsied either when tumors became palpable or the mice became moribund. It has previously been shown that castration of young TRAMP mice delays primary tumor growth [69], and we similarly observed prolonged survival in TRAMP single-Tg mice that had been castrated versus sham-operated (291 ± 42 (mean ± SEM) days survival post-surgery versus 147 ± 15 days, respectively; $p < 0.01$, one-way ANOVA plus Tukey's post-test). Further, 3 of the 8 castrated TRAMP mice (38%) did not develop detectable tumors, in contrast to only 1 of the 7 controls (14%). In contrast, castration did not increase mean survival in G2-TP mice (178 ± 27 in castrated versus 145 ± 10 days in sham controls; non-significant, one-way ANOVA plus Tukey's post-test). Further, the incidence of metastasis was similar in castrated and sham control G2-TP mice (9/19 (47%) and 12/30 (40%), respectively).

These observations were consistent with the possibility that the GRK2-DN transgene, that suppresses AR, indeed programs non-AR-driven disease. Nevertheless, this experiment was complicated because 6/19 (32%) of the castrated G2-TP mice became moribund prior to developing detectable tumors (compared to 2/29 (7%) of the sham control G2-TP mice). Although we cannot rule out that these castrated G2-TP mice harbored undetected metastasis in critical anatomical sites, it is perhaps more plausible that they developed tumor-unrelated side effects such as neurological defects [70].

Given that GRK2-DN single-Tg prostates do not form tumors but exhibit reduced AR and AR target gene expression (Figs. 4d, 5), we reasoned that these mice would provide a more

direct means to test the role of GRK2 in enforcing the AR-driven state. Specifically, castration in WT mice leads to involution of the prostate within 10 days [71], and thus resistance to castration-induced involution in GRK2-DN single-Tg prostates would indicate that blockade of GRK2 function programs the non-AR-driven state. Importantly, this alternate approach avoids the necessity of waiting several months for tumors – as well as complicating castration-associated side effects – to develop.

As expected, prostate weights in control WT mice were reduced 2.2-fold 10 days post-castration compared to sham controls ($p < 0.001$, one-way ANOVA plus Tukey's post-test). In contrast, castration only minimally reduced prostate weight in GRK2-DN mice (1.3-fold, statistically non-significant (ns)) (Fig. 8). Importantly, the impact of castration on reducing prostate weight was less in GRK2-DN mice compared to WT (the mean difference between sham and castration surgeries was significantly greater in WT compared to GRK2-DN; interaction p value = 0.04, 2-factor ANOVA). Taken together, these data point to a role for GRK2 in supporting AR expression and enforcing AR-dependence via a mechanism that can act independently of tumor formation.

Discussion

GRK2 regulates the aggressiveness of prostate and other tumors [47–51, 53]. For instance, directly blocking G protein signaling (that is naturally inhibited by GRK2) diminishes the in vivo tumor-forming potential of the castration-resistant human prostate tumor cell line PC-3 [52]. Conversely, in primary human prostate tumors, GRK2 expression decreases with advancing Gleason score [54]. GRK2 can be regulated by RKIP, that also regulates mitogenic MAPK signaling [72] and inflammation [73]. RKIP is expressed in healthy human prostate epithelia, but diminishes in primary prostate tumors and is absent in metastasis [74]. Further, RKIP ablation accelerates tumorigenesis in TRAMP mice [44]. We therefore hypothesized that expressing a dominant-negative GRK2 (GRK2-DN) in the prostate would reveal natural cancer progression pathways by amplifying signals triggered by ambient GPCR ligands that promote cell migration and hence metastasis. Indeed, although the GRK2-DN transgene did not by itself induce oncogenesis (Figs. 1d and 4a), it dramatically increased the incidence of metastasis when crossed to TRAMP mice that express SV40 T antigen (Fig. 3a). Further, double transgenic (G2-TP) mice often harbored metastasis in visceral organs (Fig. 3b, c).

Another notable aspect of the G2-TP primary tumors and metastasis is that they appear to be castrate-resistant. Further, although previous in vitro studies support the possibility that augmented G protein activity in prostate tumor cells (as would be expected following the loss of GRK2 function, Fig. 1b–d) facilitates androgen-independent AR activation and hence maintains AR-driven tumor growth in the face of androgen deprivation [75], in the current study G2-TP primary tumors and metastasis unexpectedly displayed a non-AR-driven profile: reduced expression of AR (Fig. 4d), AR target genes (Fig. 5) and 5α-reductase (Fig. 6), but increased NEPC marker mRNAs (Fig. 7). In fact, our current results are consistent with a previous study demonstrating that low β-arrestin expression in human prostate tumor cell lines is associated with diminished AR expression and activity [76]. Thus, since β-arrestin acts downstream of GRK2 in regulating GPCR signaling [45, 46], diminished

activity of either regulator would have a similar effect in disinhibiting canonical GPCR signaling and hence programming the non-AR-driven state.

Transition from the AR-driven to non-AR-driven state is normally associated with advanced stages of prostate cancer progression. Although the mechanisms underlying this switch are not fully understood, it has been shown that augmented PI3K activity, consequent to PTEN tumor suppressor loss, suppresses AR [29]. In contrast, GRK2-DN-mediated AR suppression appears to occur through a PTEN-independent mechanism. Thus, GRK2-DN single-Tg prostates, which express PTEN mRNA (not shown) and do not form tumors (Fig. 1d, 4a), express reduced AR and AR target genes compared to WT (Figs. 4d, 5). Further, GRK2-DN prostates resist castration-induced involution (Fig. 8). Together, these results support a role for GRK2 in enforcing AR-dependence in healthy prostate by dampening GPCR-linked pathways that would otherwise program the non-AR-driven state. The loss of prostatic GRK2 function may thus only have a minor impact in men who do not have cancer. For instance, diminished GRK2 has been observed in biopsies of human benign prostate hyperplasia [54]. Nevertheless, GRK2 loss may predispose prostate epithelial cells towards rapid tumor progression following a subsequent oncogenic event. In this regard, an interesting aspect of our model is that owing to the GRK2-DN transgene being an AR target, its own expression is downregulated in G2-TP compared to TRAMP prostate tumors (Fig. 4). Consistent with this, we did not detect pCREB immunoreactivity in G2-TP liver metastasis (not shown), suggesting that continued disinhibition of GPCR signaling is not required to maintain the advanced disease state once it has become established. Taken together, transient loss of GRK2 function appears sufficient to program the non-AR-driven state.

In summary, the current study supports a role for prostatic GRK2 in regulating a GPCR-mediated signaling pathway(s) that would otherwise suppress AR, hence maintaining the AR-driven state. Conversely, the loss of prostatic GRK2 function amplifies GPCR-G protein signaling that programs the non-AR-driven state. The GRK2-DN model might thus provide a platform for future studies aimed at identifying the relevant GPCR ligand(s) and signaling pathways. Finally, the current findings also raise the prospect that augmenting GRK2 activity during androgen deprivation therapy might be a viable strategy for preventing the development of non-AR-driven prostate cancer.

Materials and methods

Mouse care, tumor monitoring and surgery

Mice were fed *ad libitum* and housed in Center for Comparative Medicine at UConn Health, Farmington, CT. All experimental protocols conform to federal regulatory standards, and were approved by the UConn Health Institutional Animal Care Committee (IACUC). Mice were euthanized and necropsied when they became moribund or their tumors became palpable. Castration surgeries were performed on 3–5 month-old male mice using sterilized instruments on mice anesthetized with ketamine/xylazine: the scrotal sac was shaved and then sterilized with Betadine followed by 70% ethanol, and then a small (~8 mm) incision was made to allow removal of the testes, which was subsequently closed with sutures. Sham controls received incisions and sutures, but their testes were left intact. Mice within a given

genotype (WT, GRK2-DN, TRAMP or G2-TP) were randomized with regard to receiving castration or sham surgeries. Mice were euthanized and excluded from the analyses if they experienced complications within the first several days following surgery (e.g., if the sutures did not hold).

Animal models

The PB-GRK2-DN transgene was constructed by ligating the GRK2-DN cDNA (βARK-K220R) [55] between the ARR_2PB small composite probasin promoter [56] and the SV40 small T antigen 3'UTR (containing splice and polyadenylation sequences). The resulting PB-GRK2-DN expression cassette (Fig. 1a) was microinjected into fertilized C57BL/6 embryos at the UConn Health Center for Mouse Genome Modification. TRAMP and non-transgenic (WT) mice were also on the C57BL/6 background.

qRT-PCR

RNA was extracted from the indicated tissues using an RNeasy Mini Kit (QIAGEN), and then reverse transcribed using an iScript cDNA Synthesis Kit and analyzed by qRT-PCR using SSoAdvanced Universal SYBR Green Supermix on a CFX96 Real-Time System C1000 Touch Thermal Cycler (all from Bio-Rad). Data were normalized to β-actin. The following primers were used: β-actin forward, 5'-AAGGCCAACCGTGAAAAGAT and reverse, 5'-GTGGTACGACCAGAGGCATAC [77]; Ki67 forward, 5'-ATCATTGACCGCTCCTTTAGGT and reverse, 5'- GCTCGCCTTGATGGTTCCT; transgene forward, 5'- AAGCTCTAAGATTCCAACCTATGG and reverse, 5'-AGCCTCATCATCACTAGATGGC; AR forward, 5'-TGCTGCTCTTCAGCATTATTCCAGT and reverse, 5'-GGTTTTGGGTATTAGGGTTTCCAAA; Nkx3–1 forward, 5'-GACTGTGAACATAATCCAGGGG and reverse, 5'- TGATGGCTGAACTTCCTCTCC' Tmprss2 forward 5'- CAGTCTGAGCACATCTGTCCT and reverse, 5'-CTCGGAGCATACTGAGGCA; CXCR4 forward, 5'-GAAGTGGGTTCTGGAGACTATG and reverse, 5'-TTGCCGACTATGCCAGTCAAG; SRD5A1 forward, 5'-GCGAGGCAGCATCATCAGT and reverse, 5'-GACACTCAGCTTATGGAAGACAACA; SRD5A2 forward, 5'-TGGGTCTCTTCTCCGCACAT and reverse, 5'-GCCTCTGGTGAGCAATGAGTAA; Aurora Kinase A forward, 5'-CTGGATGCTGCAAACGGATAG and reverse, 5'- CGAAGGGAACAGTGGTCTTAACA; Chromogranin A forward, 5'-ATCCTCTCTATCCTGCGACAC and reverse, 5'-GGGCTCTGGTTCTCAAACACT; Synaptophysin forward, 5'-CAGTTCCGGGTGGTCAAGG and reverse, 5- ACTCTCCGTCTTGTTGGCAC.

Western blotting

Prostates were lysed in lysis buffer (50 mM Tris–HCl, pH 7.4, 150 mM NaCl, 1% Triton X-100, 1 mM EDTA, 5 mM NaF, 2 mM sodium orthovanadate, 1 mM PMSF, 1× complete protease inhibitors), boiled at 100°C for 10 min in Laemmli buffer (BioRad) with 2-mercaptoethanol, and run on a 4–20% gradient SDS-PAGE gel (BioRad). Following transfer to a nitrocellulose membrane, blots were probed with rabbit anti-mouse mAbs to CREB or pCREB (Cat #9197S and 9198, respectively, Cell Signaling), rabbit anti-mouse polyclonal Ab to pPKA C (Cat #4781S, Cell Signaling) or rabbit anti-mouse polyclonal IgG to β-

tubulin (Cat #2146S, Cell Signaling) followed with mouse anti-rabbit HRP conjugate (Cat #SC-2357, Santa Cruz), and developed using an ECL plus chemiluminescence kit (Cat#32132, Thermo Fisher Scientific). B16-F10 melanoma cells (Cat#CRL-6475, ATCC) treated 1 h with or without 25 μM forskolin (FSK, adenylyl cyclase activator) served as pCREB positive and negative controls, respectively. Protein quantification was performed using GeneTools software (Syngene).

Histology and immunohistochemistry

Histological analyses were performed at the UConn Health Research Histology Core. Hematoxylin and eosin (H & E) staining was performed on 8 micron formalin-fixed paraffin-embedded tissue sections. Immunohistochemistry was performed on similar sections that were stained with hematoxylin and either rat anti-mouse mAb to Ki67 (Cat #M7249, Dako) or rabbit anti-mouse mAb to pCREB (Cat #9198, Cell Signaling) followed by HRP-conjugated secondary antibodies (Dako), and then developed using a VECTASTAIN Elite ABC-HRP kit (LSBio).

Statistical analyses

GraphPad Prism was used to generate all of the graphs and to perform most of the statistical analyses (indicated in the text and figure legends) except for the following analyses that were performed using SAS software: p values in Fig. 6 were calculated using TrendTest to compare *Srd5a* expression across the multiple groups representing advancing disease stages. Additionally, in Fig. 8 a 2-factor ANOVA was fitted to assess differences in Day 10 prostate weights with main effects of treatment (sham versus castration) and methods (WT and GRK2-DN) and the (treatment ´ method) interaction. A significant p value for the interaction term indicates that treatment is statistically different across method type. Sample sizes are indicated in the corresponding text and or figure legends, and were chosen based on the power to detect significant differences ($p < 0.05$) between either WT and GRK2-DN prostates (Western blot analyses), castrated versus sham-operated TRAMP mice (survival) or castrated versus sham-operated WT mice (prostate involution). The investigator was not blinded during either group allocation or in assessing experimental outcomes.

Acknowledgements

This work was supported by National Institutes of Health Grants R01CA109339 and R01AI094640 (to A.J.A. and A.T.V.) and by the Carole and Ray Neag Comprehensive Cancer Center. The authors thank Dr. Jeffrey Benovic for providing the GRK2-DN (βARK-K220R) construct, Dr. Robert Matusik for providing the ARR_2PB construct as well as helpful discussions and critical reading of the manuscript, Dr. Stefan Brocke for advice regarding in vitro forskolin stimulations, and Dr. Christopher Bonin for editing the manuscript.

References

1. Siegel RL, Miller KD, Jemal A. Cancer statistics, 2019. CA Cancer J Clin. 2019;69:7–34. [PubMed: 30620402]
2. Denmeade SR, Isaacs JT. A history of prostate cancer treatment. Nat Rev Cancer. 2002;2:389–96. [PubMed: 12044015]
3. Watson PA, Arora VK, Sawyers CL. Emerging mechanisms of resistance to androgen receptor inhibitors in prostate cancer. Nat Rev Cancer. 2015;15:701–11. [PubMed: 26563462]

4. Dehm SM, Schmidt LJ, Heemers HV, Vessella RL, Tindall DJ. Splicing of a novel androgen receptor exon generates a constitutively active androgen receptor that mediates prostate cancer therapy resistance. Cancer Res. 2008;68:5469–77. [PubMed: 18593950]
5. Palmgren JS, Karavadia SS, Wakefield MR. Unusual and underappreciated: small cell carcinoma of the prostate. Semin Oncol. 2007;34:22–9. [PubMed: 17270662]
6. Beltran H, Rickman DS, Park K, Chae SS, Sboner A, MacDonald TY, et al. Molecular characterization of neuroendocrine prostate cancer and identification of new drug targets. Cancer Discov. 2011;1:487–95. [PubMed: 22389870]
7. Bluemn EG, Coleman IM, Lucas JM, Coleman RT, Hernandez-Lopez S, Tharakan R, et al. Androgen Receptor Pathway-Independent Prostate Cancer Is Sustained through FGF Signaling. Cancer Cell. 2017;32:474–89 e6. [PubMed: 29017058]
8. Hirano D, Okada Y, Minei S, Takimoto Y, Nemoto N. Neuroendocrine differentiation in hormone refractory prostate cancer following androgen deprivation therapy. Eur Urol. 2004;45:586–92; discussion 92. [PubMed: 15082200]
9. Alanee S, Moore A, Nutt M, Holland B, Dynda D, El-Zawahry A, et al. Contemporary Incidence and Mortality Rates of Neuroendocrine Prostate Cancer. Anticancer Res. 2015;35:4145–50. [PubMed: 26124369]
10. Zou M, Toivanen R, Mitrofanova A, Floc'h N, Hayati S, Sun Y, et al. Transdifferentiation as a Mechanism of Treatment Resistance in a Mouse Model of Castration-resistant Prostate Cancer. Cancer Discov. 2017.
11. Gandaglia G, Karakiewicz PI, Briganti A, Passoni NM, Schiffmann J, Trudeau V, et al. Impact of the Site of Metastases on Survival in Patients with Metastatic Prostate Cancer. Eur Urol. 2014.
12. Drake CG. Visceral metastases and prostate cancer treatment: 'die hard,' 'tough neighborhoods,' or 'evil humors'? Oncology (Williston Park). 2014;28:974–80. [PubMed: 25403629]
13. Hodi FS, O'Day SJ, McDermott DF, Weber RW, Sosman JA, Haanen JB, et al. Improved survival with ipilimumab in patients with metastatic melanoma. N Engl J Med. 2010;363:711–23. [PubMed: 20525992]
14. Kwon ED, Drake CG, Scher HI, Fizazi K, Bossi A, van den Eertwegh AJ, et al. Ipilimumab versus placebo after radiotherapy in patients with metastatic castration-resistant prostate cancer that had progressed after docetaxel chemotherapy (CA184–043): a multicentre, randomised, double-blind, phase 3 trial. Lancet Oncol. 2014;15:700–12. [PubMed: 24831977]
15. Aggarwal R, Huang J, Alumkal JJ, Zhang L, Feng FY, Thomas GV, et al. Clinical and Genomic Characterization of Treatment-Emergent Small-Cell Neuroendocrine Prostate Cancer: A Multi-institutional Prospective Study. J Clin Oncol. 2018;36:2492–503. [PubMed: 29985747]
16. Lee JK, Phillips JW, Smith BA, Park JW, Stoyanova T, McCaffrey EF, et al. N-Myc Drives Neuroendocrine Prostate Cancer Initiated from Human Prostate Epithelial Cells. Cancer Cell. 2016;29:536–47. [PubMed: 27050099]
17. Carver BS. Defining and Targeting the Oncogenic Drivers of Neuroendocrine Prostate Cancer. Cancer Cell. 2016;29:431–2. [PubMed: 27070695]
18. Bishop JL, Thaper D, Vahid S, Davies A, Ketola K, Kuruma H, et al. The Master Neural Transcription Factor BRN2 Is an Androgen Receptor-Suppressed Driver of Neuroendocrine Differentiation in Prostate Cancer. Cancer Discov. 2017;7:54–71. [PubMed: 27784708]
19. Greenberg NM, DeMayo F, Finegold MJ, Medina D, Tilley WD, Aspinall JO, et al. Prostate cancer in a transgenic mouse. Proc Natl Acad Sci U S A. 1995;92:3439–43. [PubMed: 7724580]
20. Taylor BS, Schultz N, Hieronymus H, Gopalan A, Xiao Y, Carver BS, et al. Integrative genomic profiling of human prostate cancer. Cancer Cell. 2010;18:11–22. [PubMed: 20579941]
21. Cancer Genome Atlas Research N. The Molecular Taxonomy of Primary Prostate Cancer. Cell. 2015;163:1011–25. [PubMed: 26544944]
22. Wang S, Gao J, Lei Q, Rozengurt N, Pritchard C, Jiao J, et al. Prostate-specific deletion of the murine Pten tumor suppressor gene leads to metastatic prostate cancer. Cancer Cell. 2003;4:209–21. [PubMed: 14522255]
23. Whang YE, Wu X, Suzuki H, Reiter RE, Tran C, Vessella RL, et al. Inactivation of the tumor suppressor PTEN/MMAC1 in advanced human prostate cancer through loss of expression. Proc Natl Acad Sci U S A. 1998;95:5246–50. [PubMed: 9560261]

24. Han G, Foster BA, Mistry S, Buchanan G, Harris JM, Tilley WD, et al. Hormone status selects for spontaneous somatic androgen receptor variants that demonstrate specific ligand and cofactor dependent activities in autochthonous prostate cancer. J Biol Chem. 2001;276:11204–13. [PubMed: 11063747]
25. Drake CG, Doody AD, Mihalyo MA, Huang CT, Kelleher E, Ravi S, et al. Androgen ablation mitigates tolerance to a prostate/prostate cancer-restricted antigen. Cancer Cell. 2005;7:239–49. [PubMed: 15766662]
26. Savage PA, Vosseller K, Kang C, Larimore K, Riedel E, Wojnoonski K, et al. Recognition of a ubiquitous self antigen by prostate cancer-infiltrating CD8+ T lymphocytes. Science. 2008;319:215–20. [PubMed: 18187659]
27. Malchow S, Leventhal DS, Nishi S, Fischer BI, Shen L, Paner GP, et al. Aire-dependent thymic development of tumor-associated regulatory T cells. Science. 2013;339:1219–24. [PubMed: 23471412]
28. Hurwitz AA, Foster BA, Kwon ED, Truong T, Choi EM, Greenberg NM, et al. Combination immunotherapy of primary prostate cancer in a transgenic mouse model using CTLA-4 blockade. Cancer Res. 2000;60:2444–8. [PubMed: 10811122]
29. Carver BS, Chapinski C, Wongvipat J, Hieronymus H, Chen Y, Chandarlapaty S, et al. Reciprocal feedback regulation of PI3K and androgen receptor signaling in PTEN-deficient prostate cancer. Cancer Cell. 2011;19:575–86. [PubMed: 21575859]
30. Mulholland DJ, Tran LM, Li Y, Cai H, Morim A, Wang S, et al. Cell autonomous role of PTEN in regulating castration-resistant prostate cancer growth. Cancer Cell. 2011;19:792–804. [PubMed: 21620777]
31. Gingrich JR, Barrios RJ, Morton RA, Boyce BF, DeMayo FJ, Finegold MJ, et al. Metastatic prostate cancer in a transgenic mouse. Cancer Res. 1996;56:4096–102. [PubMed: 8797572]
32. Chiaverotti T, Couto SS, Donjacour A, Mao JH, Nagase H, Cardiff RD, et al. Dissociation of epithelial and neuroendocrine carcinoma lineages in the transgenic adenocarcinoma of mouse prostate model of prostate cancer. Am J Pathol. 2008;172:236–46. [PubMed: 18156212]
33. Grabowska MM, DeGraff DJ, Yu X, Jin RJ, Chen Z, Borowsky AD, et al. Mouse models of prostate cancer: picking the best model for the question. Cancer Metastasis Rev. 2014;33:377–97. [PubMed: 24452759]
34. Xu LL, Stackhouse BG, Florence K, Zhang W, Shanmugam N, Sesterhenn IA, et al. PSGR, a novel prostate-specific gene with homology to a G protein-coupled receptor, is overexpressed in prostate cancer. Cancer Res. 2000;60:6568–72. [PubMed: 11118034]
35. Yowell CW, Daaka Y. G protein-coupled receptors provide survival signals in prostate cancer. Clin Prostate Cancer. 2002;1:177–81. [PubMed: 15046693]
36. Daaka Y G proteins in cancer: the prostate cancer paradigm. Sci STKE. 2004;2004:re2. [PubMed: 14734786]
37. Furusato B, Mohamed A, Uhlen M, Rhim JS. CXCR4 and cancer. Pathol Int. 2010;60:497–505. [PubMed: 20594270]
38. Lee H, Deng J, Kujawski M, Yang C, Liu Y, Herrmann A, et al. STAT3-induced S1PR1 expression is crucial for persistent STAT3 activation in tumors. Nat Med. 2010;16:1421–8. [PubMed: 21102457]
39. Qiao J, Grabowska MM, Forestier-Roman IS, Mirosevich J, Case TC, Chung DH, et al. Activation of GRP/GRP-R signaling contributes to castration-resistant prostate cancer progression. Oncotarget. 2016;7:61955–69. [PubMed: 27542219]
40. Zhou Z, Flesken-Nikitin A, Corney DC, Wang W, Goodrich DW, Roy-Burman P, et al. Synergy of p53 and Rb deficiency in a conditional mouse model for metastatic prostate cancer. Cancer Res. 2006;66:7889–98. [PubMed: 16912162]
41. Ding Z, Wu CJ, Chu GC, Xiao Y, Ho D, Zhang J, et al. SMAD4-dependent barrier constrains prostate cancer growth and metastatic progression. Nature. 2011;470:269–73. [PubMed: 21289624]
42. Ding Z, Wu CJ, Jaskelioff M, Ivanova E, Kost-Alimova M, Protopopov A, et al. Telomerase reactivation following telomere dysfunction yields murine prostate tumors with bone metastases. Cell. 2012;148:896–907. [PubMed: 22341455]

43. Mulholland DJ, Kobayashi N, Ruscetti M, Zhi A, Tran LM, Huang J, et al. Pten loss and RAS/MAPK activation cooperate to promote EMT and metastasis initiated from prostate cancer stem/progenitor cells. Cancer Res. 2012;72:1878–89. [PubMed: 22350410]
44. Escara-Wilke J, Keller JM, Ignatoski KM, Dai J, Shelley G, Mizokami A, et al. Raf kinase inhibitor protein (RKIP) deficiency decreases latency of tumorigenesis and increases metastasis in a murine genetic model of prostate cancer. Prostate. 2015;75:292–302. [PubMed: 25327941]
45. Pitcher JA, Freedman NJ, Lefkowitz RJ. G protein-coupled receptor kinases. Annu Rev Biochem. 1998;67:653–92. [PubMed: 9759500]
46. Komolov KE, Benovic JL. G protein-coupled receptor kinases: Past, present and future. Cell Signal. 2018;41:17–24. [PubMed: 28711719]
47. Nogues L, Reglero C, Rivas V, Neves M, Penela P, Mayor F Jr. G-Protein-Coupled Receptor Kinase 2 as a Potential Modulator of the Hallmarks of Cancer. Mol Pharmacol. 2017;91:220–8. [PubMed: 27895163]
48. Fu X, Koller S, Abd Alla J, Quitterer U. Inhibition of G-protein-coupled receptor kinase 2 (GRK2) triggers the growth-promoting mitogen-activated protein kinase (MAPK) pathway. J Biol Chem. 2013;288:7738–55. [PubMed: 23362259]
49. Metaye T, Levillain P, Kraimps JL, Perdrisot R. Immunohistochemical detection, regulation and antiproliferative function of G-protein-coupled receptor kinase 2 in thyroid carcinomas. J Endocrinol. 2008;198:101–10. [PubMed: 18451066]
50. Xu ZW, Yan SX, Wu HX, Chen JY, Zhang Y, Li Y, et al. The influence of TNF-alpha and Ang II on the proliferation, migration and invasion of HepG2 cells by regulating the expression of GRK2. Cancer Chemother Pharmacol. 2017;79:747–58. [PubMed: 28315953]
51. Hu M, Wang C, Li W, Lu W, Bai Z, Qin D, et al. A KSHV microRNA Directly Targets G Protein-Coupled Receptor Kinase 2 to Promote the Migration and Invasion of Endothelial Cells by Inducing CXCR2 and Activating AKT Signaling. PLoS Pathog. 2015;11:e1005171. [PubMed: 26402907]
52. Bookout AL, Finney AE, Guo R, Peppel K, Koch WJ, Daaka Y. Targeting Gbetagamma signaling to inhibit prostate tumor formation and growth. J Biol Chem. 2003;278:37569–73. [PubMed: 12869546]
53. Wang ZQ, He CY, Hu L, Shi HP, Li JF, Gu QL, et al. Long noncoding RNA UCA1 promotes tumour metastasis by inducing GRK2 degradation in gastric cancer. Cancer Lett. 2017;408:10–21. [PubMed: 28843497]
54. Prowatke I, Devens F, Benner A, Grone EF, Mertens D, Grone HJ, et al. Expression analysis of imbalanced genes in prostate carcinoma using tissue microarrays. Br J Cancer. 2007;96:82–8. [PubMed: 17146477]
55. Kong G, Penn R, Benovic JL. A beta-adrenergic receptor kinase dominant negative mutant attenuates desensitization of the beta 2-adrenergic receptor. J Biol Chem. 1994;269:13084–7. [PubMed: 8175732]
56. Zhang J, Thomas TZ, Kasper S, Matusik RJ. A small composite probasin promoter confers high levels of prostate-specific gene expression through regulation by androgens and glucocorticoids in vitro and in vivo. Endocrinology. 2000;141:4698–710. [PubMed: 11108285]
57. Gingrich J, Barrios R, Foster B, Greenberg N. Pathologic progression of autochonous prostate cancer in the TRAMP model. Prostate Cancer and Prostatic Diseases. 1999;6:1–6.
58. Shaywitz AJ, Greenberg ME. CREB: a stimulus-induced transcription factor activated by a diverse array of extracellular signals. Annu Rev Biochem. 1999;68:821–61. [PubMed: 10872467]
59. Lonergan PE, Tindall DJ. Androgen receptor signaling in prostate cancer development and progression. J Carcinog. 2011;10:20. [PubMed: 21886458]
60. Greenberg NM, DeMayo FJ, Sheppard PC, Barrios R, Lebovitz R, Finegold M, et al. The rat probasin gene promoter directs hormonally and developmentally regulated expression of a heterologous gene specifically to the prostate in transgenic mice. Mol Endocrinol. 1994;8:230–9. [PubMed: 8170479]
61. He WW, Sciavolino PJ, Wing J, Augustus M, Hudson P, Meissner PS, et al. A novel human prostate-specific, androgen-regulated homeobox gene (NKX3.1) that maps to 8p21, a region frequently deleted in prostate cancer. Genomics. 1997;43:69–77. [PubMed: 9226374]

62. Bethel CR, Faith D, Li X, Guan B, Hicks JL, Lan F, et al. Decreased NKX3.1 protein expression in focal prostatic atrophy, prostatic intraepithelial neoplasia, and adenocarcinoma: association with gleason score and chromosome 8p deletion. Cancer Res. 2006;66:10683–90. [PubMed: 17108105]

63. Abate-Shen C, Banach-Petrosky WA, Sun X, Economides KD, Desai N, Gregg JP, et al. Nkx3.1; Pten mutant mice develop invasive prostate adenocarcinoma and lymph node metastases. Cancer Res. 2003;63:3886–90. [PubMed: 12873978]

64. Lin B, Ferguson C, White JT, Wang S, Vessella R, True LD, et al. Prostate-localized and androgen-regulated expression of the membrane-bound serine protease TMPRSS2. Cancer Res. 1999;59:4180–4. [PubMed: 10485450]

65. Cai J, Kandagatla P, Singareddy R, Kropinski A, Sheng S, Cher ML, et al. Androgens Induce Functional CXCR4 through ERG Factor Expression in TMPRSS2-ERG Fusion-Positive Prostate Cancer Cells. Transl Oncol. 2010;3:195–203. [PubMed: 20563261]

66. Chang KH, Li R, Papari-Zareei M, Watumull L, Zhao YD, Auchus RJ, et al. Dihydrotestosterone synthesis bypasses testosterone to drive castration-resistant prostate cancer. Proc Natl Acad Sci U S A. 2011;108:13728–33. [PubMed: 21795608]

67. Chang KH, Li R, Kuri B, Lotan Y, Roehrborn CG, Liu J, et al. A gain-of-function mutation in DHT synthesis in castration-resistant prostate cancer. Cell. 2013;154:1074–84. [PubMed: 23993097]

68. Kaplan-Lefko PJ, Chen TM, Ittmann MM, Barrios RJ, Ayala GE, Huss WJ, et al. Pathobiology of autochthonous prostate cancer in a pre-clinical transgenic mouse model. Prostate. 2003;55:219–37. [PubMed: 12692788]

69. Gingrich JR, Barrios RJ, Kattan MW, Nahm HS, Finegold MJ, Greenberg NM. Androgen-independent prostate cancer progression in the TRAMP model. Cancer Res. 1997;57:4687–91. [PubMed: 9354422]

70. Khasnavis S, Ghosh A, Roy A, Pahan K. Castration induces Parkinson disease pathologies in young male mice via inducible nitric-oxide synthase. J Biol Chem. 2013;288:20843–55. [PubMed: 23744073]

71. Sugimura Y, Cunha GR, Donjacour AA. Morphological and histological study of castration-induced degeneration and androgen-induced regeneration in the mouse prostate. Biol Reprod. 1986;34:973–83. [PubMed: 3730489]

72. Lorenz K, Lohse MJ, Quitterer U. Protein kinase C switches the Raf kinase inhibitor from Raf-1 to GRK-2. Nature. 2003;426:574–9. [PubMed: 14654844]

73. Wright KT, Vella AT. RKIP contributes to IFN-gamma synthesis by CD8+ T cells after serial TCR triggering in systemic inflammatory response syndrome. J Immunol. 2013;191:708–16. [PubMed: 23761631]

74. Fu Z, Smith PC, Zhang L, Rubin MA, Dunn RL, Yao Z, et al. Effects of raf kinase inhibitor protein expression on suppression of prostate cancer metastasis. J Natl Cancer Inst. 2003;95:878–89. [PubMed: 12813171]

75. Kasbohm EA, Guo R, Yowell CW, Bagchi G, Kelly P, Arora P, et al. Androgen receptor activation by G(s) signaling in prostate cancer cells. J Biol Chem. 2005;280:11583–9. [PubMed: 15653681]

76. Purayil HT, Zhang Y, Dey A, Gersey Z, Espana-Serrano L, Daaka Y. Arrestin2 modulates androgen receptor activation. Oncogene. 2015;34:3144–51. [PubMed: 25109335]

77. Tsurutani N, Mittal P, St Rose MC, Ngoi SM, Svedova J, Menoret A, et al. Costimulation Endows Immunotherapeutic CD8 T Cells with IL-36 Responsiveness during Aerobic Glycolysis. J Immunol. 2016;196:124–34. [PubMed: 26573834]

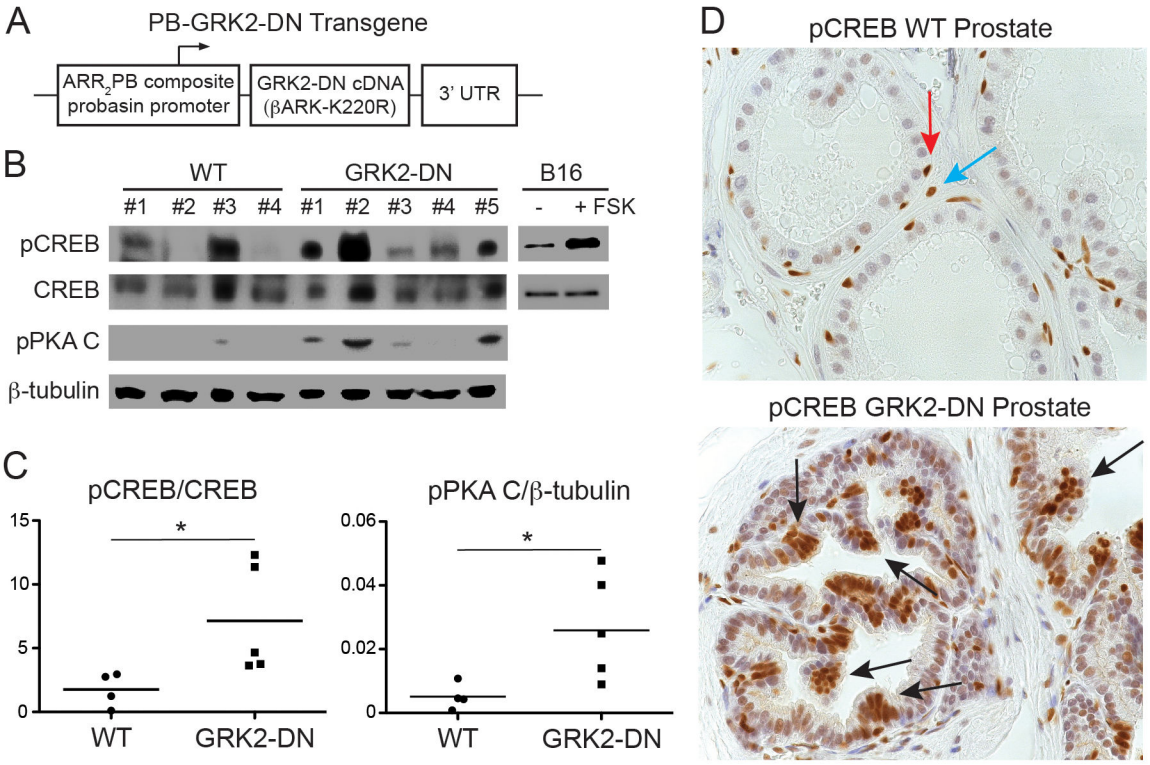

Fig. 1.

GRK2-DN transgenic mice. **a** The PB-GRK2-DN transgene was constructed by cloning the GRK2-DN cDNA (βARK-K220R) [55] between the ARR_2PB small composite probasin promoter [56] and the SV40 small T antigen 3'UTR. **b** Loss of GRK2 function disinhibits canonical GPCR signaling. Western blot for pCREB (Ser133), CREB, pPKA C and β-tubulin on cell lysates of non-Tg (WT) and GRK2-DN prostates (4 and 5 separate mouse replicates, respectively, all 3–4 months of age). B16-F10 melanoma cells (B16) treated 1 h −/+ 25 μg forskolin (FSK, adenylyl cyclase activator) served as pCREB negative and positive controls, respectively. Lysates were divided equally and run on three separate SDS-PAGE gels that were subsequently transferred onto nitrocellulose membranes and probed with anti-pCREB, -CREB, -pPKA C or -β-tubulin Abs as detailed in the methods. Cropped images are presented from each blot that contain the relevant band as confirmed via molecular weight size standards. Please note that pCREB, CREB and pPKA C were stained on separate blots due to their similar sizes (42–43 kDa), while CREB (43 kDa) and β-tubulin (50 kDa) were stained on the same blot. **c** Quantification of the pCREB and pPKA C bands in the WT versus GRK2-DN prostate lysates shown in b. pCREB and pPKA C band intensities quantified by GeneTools software (Syngene) were normalized to the corresponding CREB and β-tubulin values, respectively. * indicates $p < 0.05$ using an unpaired two-tailed *t* test, and F test indicated different variance for the pPKA C graph. **d** Representative pCREB IHC fields for WT (top panel) and GRK2-DN (bottom panel) prostates. The red arrow indicates a $pCREB^+$ basal epithelial cell, the blue arrow indicates a $pCREB^+$ stromal cell, and black arrows indicate patches of intense pCREB staining.

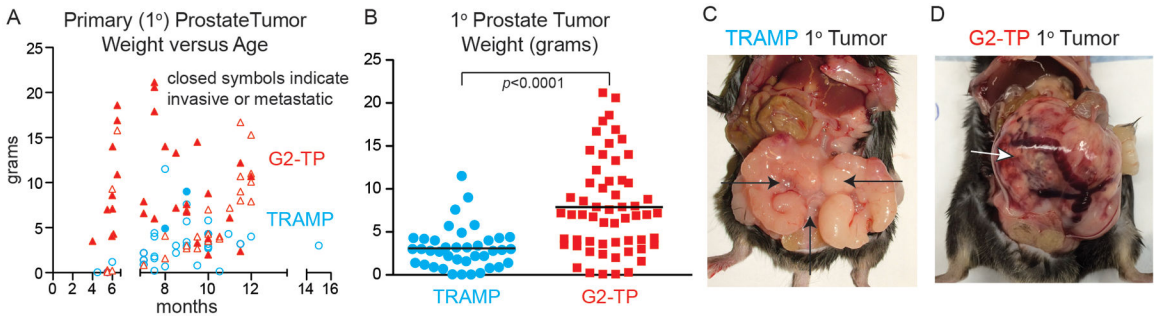

Fig. 2.

GRK2 blockade accelerates prostate tumorigenesis. **a** Age versus primary (1°) tumor weight for TRAMP ($n = 39$) and GRK2-DN × TRAMP (G2-TP, $n = 58$) mice. Closed symbols indicate metastatic or invasive 1° tumors. Not shown are single-Tg GRK2-DN mice that had no increase in prostate weight even at 20 months. **b** 1° prostate tumor weights (horizontal bars indicate means) at necropsy in the same TRAMP (mean age 8.8 ± 1.5 months) and G2-TP (8.6 ± 0.3 months) mice shown in panel a. **c** Representative TRAMP 1° prostate tumor. The vertical arrow points to the tumor, while the horizontal arrows point to the distended seminal vesicles. **d** Representative age-matched G2-TP 1° prostate tumor (white arrow).

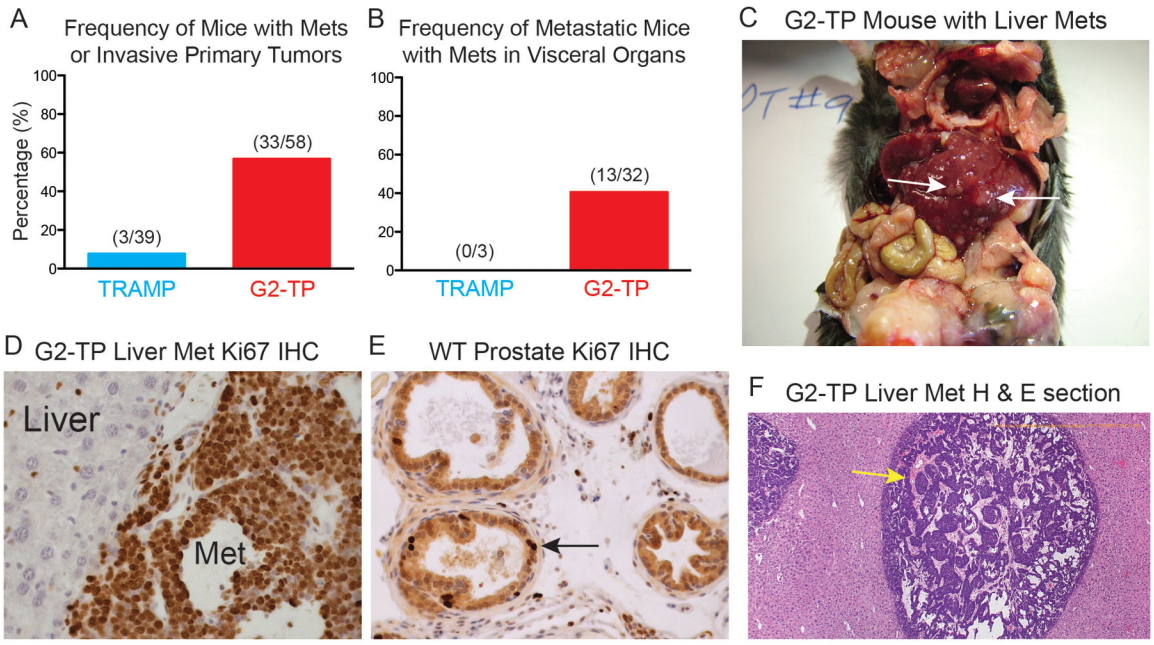

Fig. 3.

Occurrence of metastasis (abbreviated as “Mets”) in TRAMP versus G2-TP mice. **a** Percentage of TRAMP and G2-TP mice with Mets or invasive primary tumors (analyzed from the same cohorts as in Fig. 2a, b). **b** Percentage of metastatic TRAMP and G2-TP mice with visceral organ Mets. **c** G2-TP liver Mets (arrows). Representative Ki67 IHC fields of a G2-TP liver Met and adjacent liver parenchyma (**d**) and a WT prostate with a sporadic $Ki67^{+}$ epithelial cell (arrow, **e**). **f** Representative H & E stained G2-TP liver section showing a moderately differentiated Met with an arrow pointing to a gland-like structure.

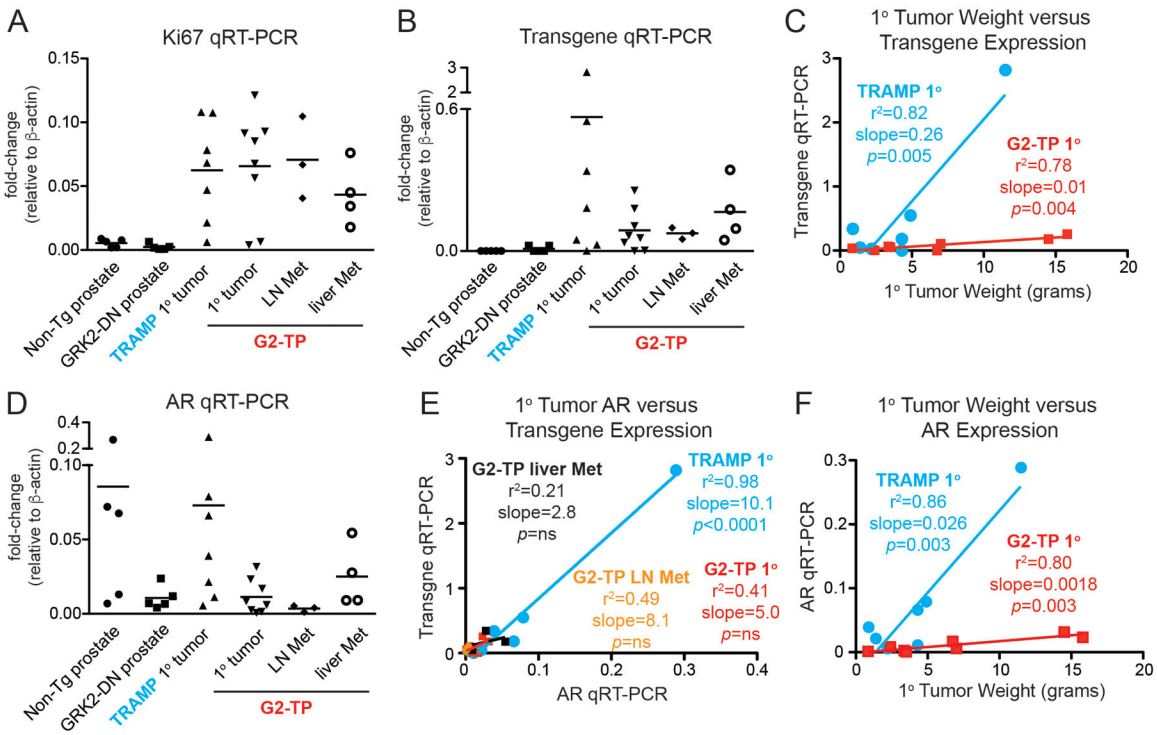

Fig. 4.

GRK2 blockade diminishes transgene and androgen receptor (AR) expression. mRNAs from non-Tg ($n = 5$) and GRK2-DN ($n = 5$) prostates, TRAMP ($n = 7$) and G2-TP ($n = 8$) 1° tumors, and G2-TP LN ($n = 3$) and liver ($n = 4$) Mets were analyzed by qRT-PCR (normalized to β-actin, with horizontal bars indicating mean values) for Ki67 (**a**), transgene (using primers specific to sequences common to both the T antigen and GRK2-DN transgenes, **b**) and AR (**d**). Linear regression analyses of TRAMP and G2-TP 1° tumor weight versus transgene (**c**) and AR mRNA expression (**f**). **e** Linear regression analysis of AR versus transgene mRNA expression in TRAMP and G2-TP 1° tumors as well as G2-TP liver and LN Mets, $p =$ ns indicates statistical non-significance. The TRAMP and G2-TP samples taken from the larger cohorts in Fig. 2a, b were similarly aged (8.1 ± 0.5 and 7.8 ± 0.9 months, respectively). Not shown is that normal LN and liver expressed baseline Ki67 mRNA levels, and expressed no transgene mRNA.

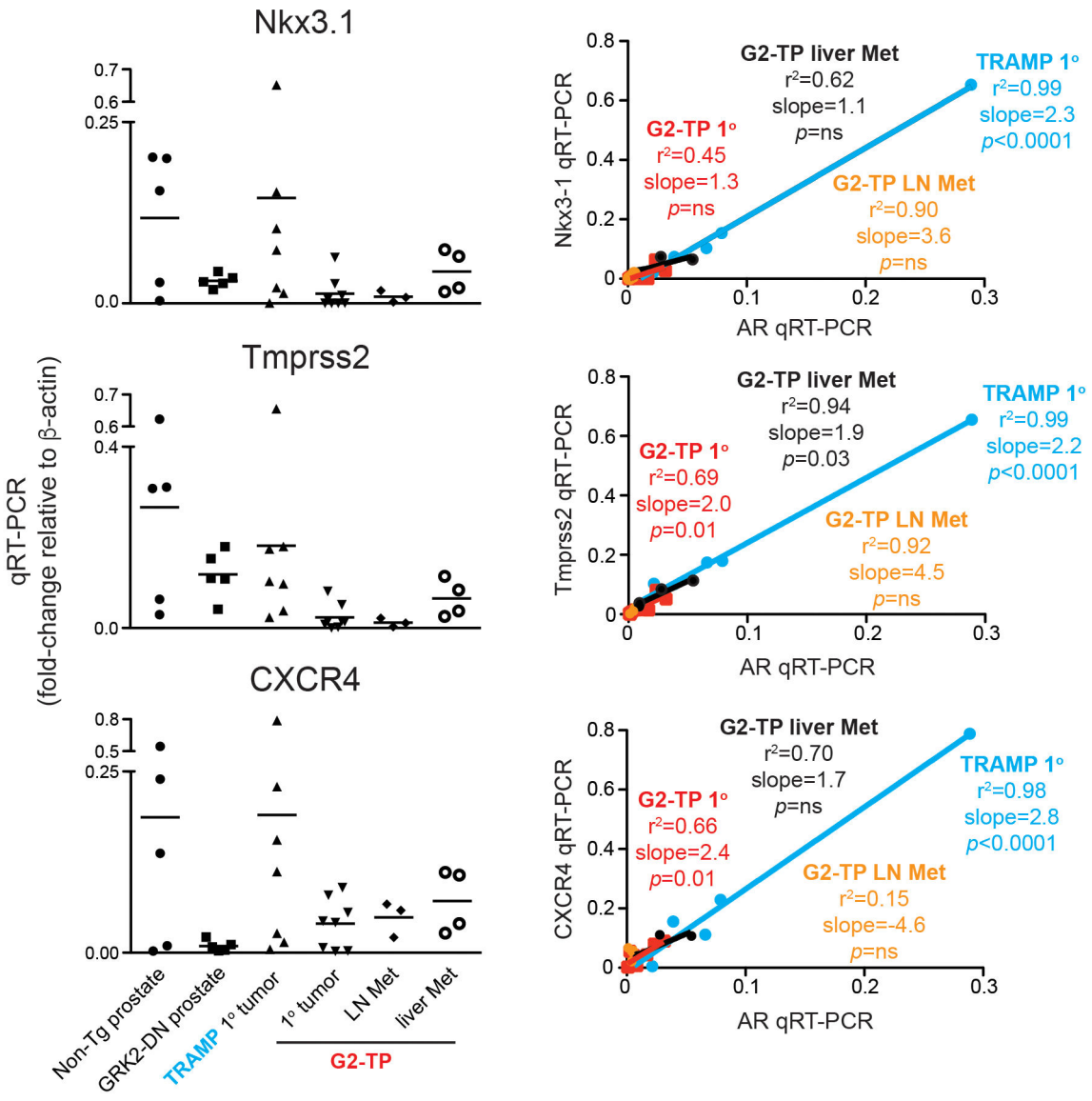

Fig. 5.

GRK2 blockade suppresses androgen-responsive target gene expression in the prostate and prostate tumors. qRT-PCR scatter plots of the AR targets Nkx3.1, Tmprss2 and CXCR4 (normalized to β-actin, and performed on the same samples as in Fig. 4) are shown on the left, and linear regression analyses of the corresponding AR target mRNA to AR mRNA (data taken from Fig. 4) are shown to the immediate right, p = ns indicates statistical non-significance.

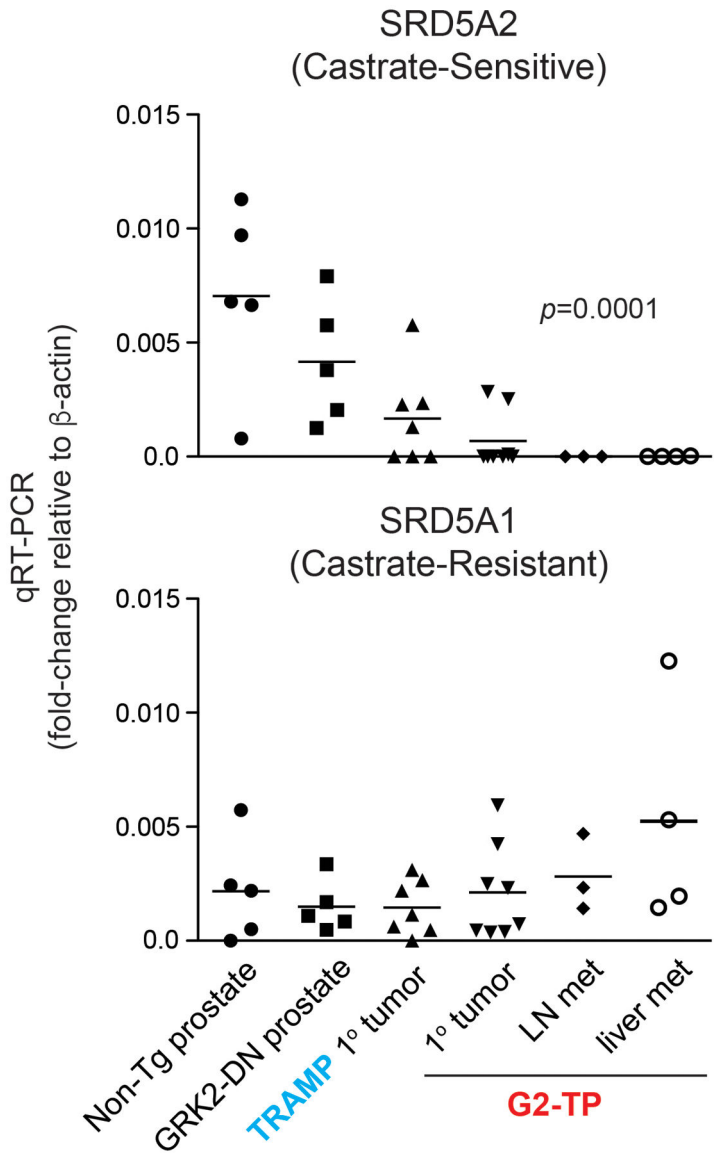

Fig. 6.

GRK2 blockade alters prostatic 5α-reductase expression. qRT-PCR analysis (normalized to β-actin) of SRD5A2 (top) and SRD5A1 (bottom) mRNAs performed on the same samples as in Figs. 4–5. The *p* value in the top panel was calculated using TrendTest.

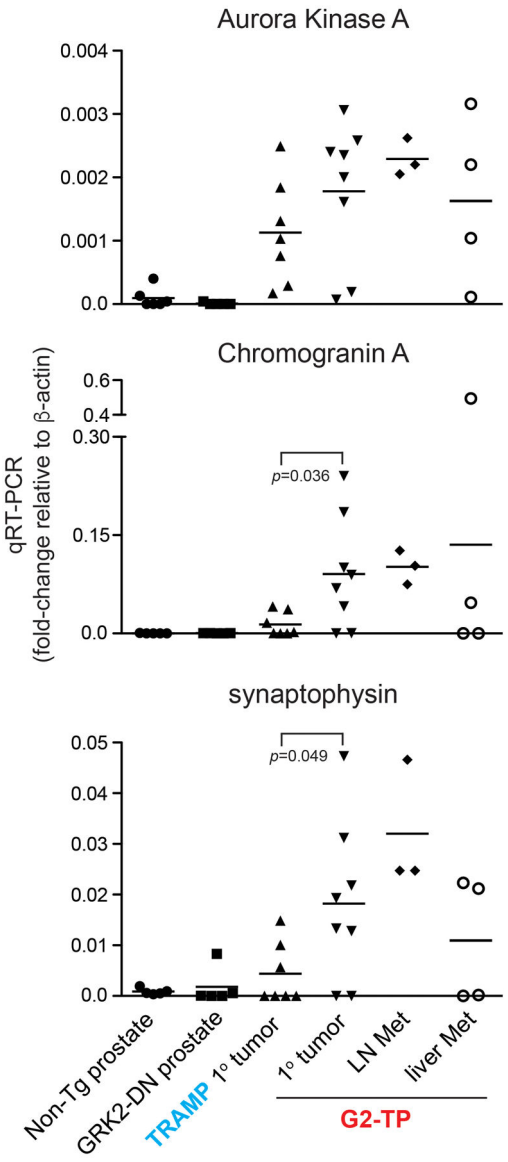

Fig. 7.

GRK2 blockade augments the expression of neuroendocrine marker mRNAs in prostate tumors. qRT-PCR analysis (normalized to β-actin) of Aurora Kinase A (top), Chromogranin A (middle) and synaptophysin (bottom) mRNAs performed on the same samples as in Figs. 4–6. Not shown is that normal LN and liver expressed negligible amounts of all three mRNAs. *P* values for TRAMP versus G2-TP comparisons were calculated using an unpaired two-tailed *t* test, where F test indicated different variance between the two groups.

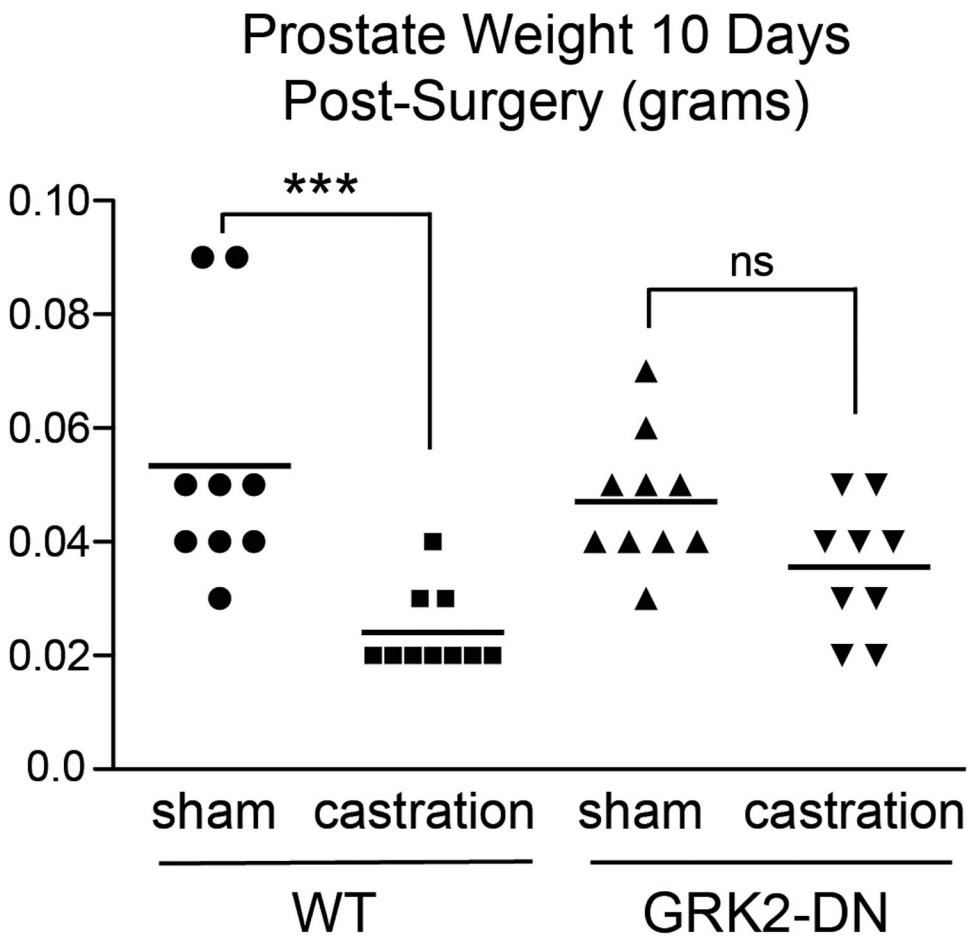

Fig. 8.

GRK2 blockade mitigates castration-induced prostate involution. GRK2-DN and WT mice (3–5 months) were castrated or sham-operated and prostate weights measured 10 days later. Data were pooled from three separate experiments that each contained all four treatment groups (n = 9–10 per group). Horizontal bars in the scatter plot indicate mean values. *** indicates $p < 0.001$ and "ns" indicates non-significant ($p > 0.05$) calculated using one-way ANOVA plus Tukey's post-test, and Bartlett's test indicated different variance between groups.